LAWRENCE
LIVERMORE
NATIONAL
LABORATORY

LLNL-JRNL-633732

Fabrication and Application of High Impedance Graded Density Impactors in Light-Gas Gun Experiments

S. J. Yep, J. L. Belof, D. A. Orlikowski, J. H. Nguyen

April 8, 2013

Review of Scientific Instruments

Disclaimer

Fabrication and Application of High Impedance Graded Density Impactors in Light-Gas Gun Experiments*

Steven J. Yep, Jonathan L. Belof, Daniel A. Orlikowski, Jeffrey H. Nguyen
Lawrence Livermore National Laboratory
Livermore, California 94551, USA
(Dated: April 4, 2013)

Recent advances in Graded Density Impactor fabrication technique have increased the maximum achievable pressure in gas-gun quasi-isentropic experiments to 5 megabars. In this report, we outline the latest methodologies and applications of graded density impactors in experiments at extreme conditions. These new graded density impactors are essentially metallic discs made of nearly one hundred layers of precisely mixed Mg, Cu and W. The density gradience in these impactors are specifically designed to generate a desired thermodynamic path designed for each experiment. We carried out a number of experiments at various pressures using these Graded Density Impactors. These experimental results and their simulations will be presented here.

PACS numbers:

INTRODUCTION

Experiments at extreme pressure-temperature conditions are often employed to replicate conditions from the deep sea to the core of the Earth and outer planetary systems [1–5]. They also yield fundamental data on the equation of state (EOS) of materials at these conditions. In dynamic compression experiments, such as light-gas gun experiments using graded density impactors (GDI), one can also access previously inaccessible regions of the phase space, study the timescale of phase transitions, and measure dynamic strength of materials along elevated isentropes [6, 7].

Currently there are four major methods to reach extremely high pressure and temperature conditions for experimental purposes: diamond anvil cells (DAC), light gas-gun, magnetic field driven and laser ablation experiments [6–13]. Each of these experimental methods has its own intrinsic preference for certain thermodynamic paths and pressure-temperature range limits. Gas-gun experiments are known for their measurement precision, especially in pressure and density where accuracy of better than 0.5% can be achieved on the Hugoniot. With GDIs, gas-gun experiments can be used to follow new thermodynamic paths and explore the phase diagram.

In previous reports, we concentrated on the fabrication of GDIs at the lower range of densities and shock impedances [14–16]. Experiments using these GDIs improved the quality of data significantly over initial experiments [6, 7]. The maximum pressure range was limited by the use of Cu and Mg in the fabrication of these impactors. Here, we report significant improvement in raising the highest impedance of the GDI that will further expand the range of accessible phase space.

MATERIALS

A complete GDI has a density range from 0.8 g/cc to 15 g/cc. These are constructed from three distinct layers: Mg-plastics, Mg-Cu, and Cu-W. Krone *et al.* [16] described in details construction of the very low density end, Mg-plastics. Martin *et al.* [14, 15] concentrated on the Mg-Cu section. We describe here the methodologies and applications for the higher density Cu-W section of the impactor. The use of these higher strength materials required a change in the fabrication technique.

Formulations

The magnesium-copper (Mg-Cu) tape casting system is a series of 41 formulations ranging from 100% magnesium and 0% copper by weight to 0% magnesium and 100% copper by weight. Individual tape castings are defined by a specific ratio of magnesium powder (20-30 μm, average particle size) to copper powder (8-11 μm, average particle size). The commercially available metallic powders are mixed together with binders and plasticizers to form a homogeneous slip. The slip is doctor bladed onto a mylar film and left to dry. Tape thicknesses of 0.106 mm to 0.072 mm are typical. Bulk densities of 3.52 g/cc to 0.90 g/cc have been attained in the raw tape castings.

The copper-tungsten (Cu-W) tape casting system consists of a series of 11 formulations ranging from 100% copper and 0% tungsten by weight to 32% copper and 68% tungsten by weight. Individual tape castings are defined by a specific ratio of copper powder (1.5-5 μm, average particle size) to tungsten powder (1-5 μm, average particle size) and manufactured similarly to the Mg-Cu tape castings. Tape thicknesses of 0.095 mm to 0.078 mm are typical. Bulk densities of 6.98 g/cc to 5.02 g/cc have been attained in the raw tape castings.

Tape Characterization

The densified properties of each tape casting formulation have been characterized. For the Mg-Cu tapes, a disk was fabricated from 50 layers of a single formulation. The layers were initially heated to 375°C in an inert environment and then hot pressed at 370°C under 40,000 lbf of uniaxial loading for 60 minutes. For the Cu-W tapes, a disk was fabricated from 55 layers of a single formulation. These layers were initially heated up to 350°C in an inert environment and then vacuum hot pressed at 950°C under 9,000 lbf of uniaxial loading for 120 minutes with a typical vacuum of $3.3 * 10^{-6}$ torr. The Cu-W tape system required a higher temperature hot press operation be developed as it would not properly densify using the Mg-Cu tape system's hot press parameters. At 370°C the magnesium would deform and creep around the copper particles in the Mg-Cu tape system. A much higher temperature process point (950°C) was required for the copper to deform and creep around the tungsten particles in the Cu-W tape system.

The bulk density of each hot pressed disk was calculated by measuring its mass, diameter, and thickness. The bulk density, ρ_{bulk}, is defined by equation 1, where the thickness, th_{avg1}, is the average of six measurements around the perimeter of the disk and one measurement at the center of the disk.

$$\rho_{bulk} = \frac{4 * mass}{\pi * diameter^2 * th_{avg1}}, \tag{1}$$

Using equation 1, the Mg-Cu tape castings achieved densities within 7% compared to their theoretical densities. The Cu-W tape castings achieved densities within 6% compared to their theoretical densities. Figure 1 summarizes the measured bulk density to the theoretical bulk density for the two tape systems.

Immersion density measurements were also taken for select Cu-W formulations such as CW3-2C and CW7-2A. When the Cu-W disks were properly densified, the calculated bulk density was consistent with the wet density measurement; percent differences of no more than 5% were observed. Wet density measurements were not undertaken with the Mg-Cu disks due to their magnesium content.

The longitudinal sound speed of each disk was measured by contact ultrasonic A-scanning employing a pulse-echo technique. A 10 MHz ultrasonic transducer with a 0.25 inch element diameter was powered by a Panametrics 5800 pulser/receiver to induce a compressional wave into the disk along its axial direction. The compression wave rebounded off any free surface and the Panametrics 5800 pulser/receiver monitored these echoes. The echo waveform was collected using a LeCroy Wavepro 950 oscilloscope set to a minimum digitizing sampling rate of 10^9 samples per second and the time of flight through the sample, t_{flight}, obtained by performing an autocorrelation on the peaks of waveform. The longitudinal sound speed, V_c, is related to the time of flight through the sample by equation 2, where the thickness, th_2, is the thickness of the sample at the location of the transducer.

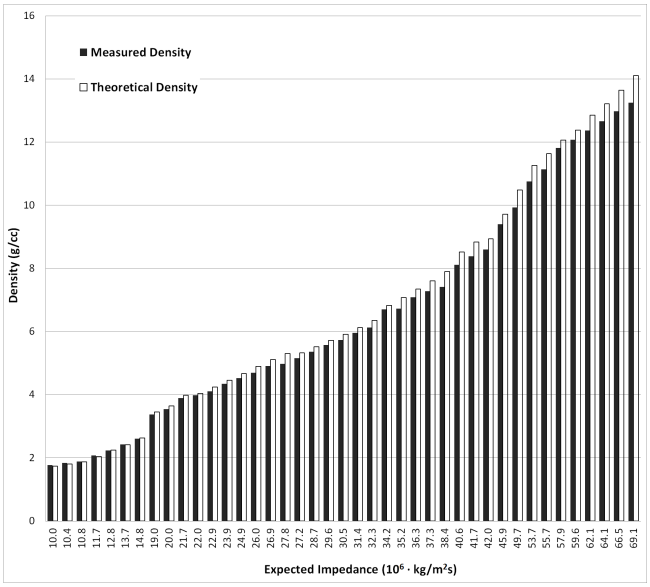

FIG. 1: Measured hot pressed densities (black bars) of the Mg-Cu tape system (expected impedance 10 to 36) and the Cu-W tape system (expected impedance 36 to 62) show all formulations are densified within 7% of their theoretical values (white bars).

$$V_c = \frac{2 * th_2}{t_{flight}} \tag{2}$$

Using the longitudinal sound speed and the bulk density, the impedance for each formulation was calculated. The acoustic impedance, Z_{ac}, is the product of the bulk density and the longitudinal sound speed as shown in equation 3.

$$z_{ac} = \rho_{bulk} V_c = \frac{4 * mass}{\pi * diameter^2 * th_{avg1}} * \frac{2 * th_2}{t_{flight}} \tag{3}$$

GDI FABRICATION METHOD

Design

Since each formulation is associated with an impedance value, a GDI can be designed to produce a tailored compression input by layering specific metal tape casting formulations. For example, a gas gun compression experiment would require the metal tape castings to be layered from lower impedances to higher impedances as shown in

figure 2. The sequence and number of layers is dependent on experiment's proposed compression profile.

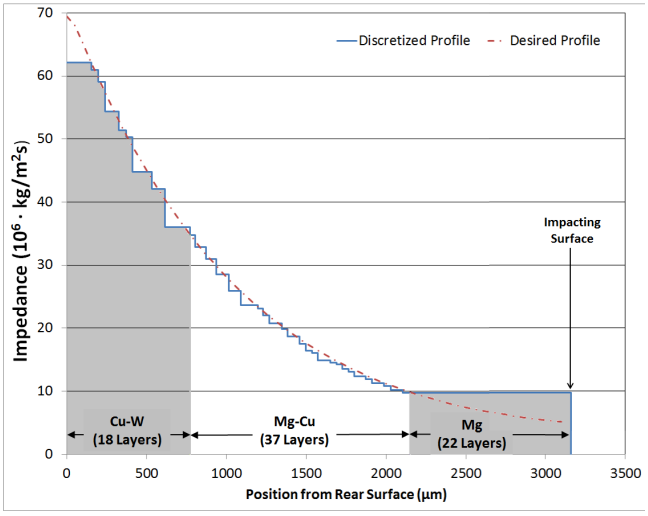

FIG. 2: Shock profile for a typical ramp compression experiment with individual tape casting layer discretization (solid blue line) shown. The full profile was divided into 3 subsequences for ease of fabrication based on material composition and thickness.

A+B Construction Method

The preferred GDI fabrication method is an A+B construction. An A+B construction indicates subsequences of the full layup (A and B) are individually processed and then these subsequences are combined later during hot pressing operations to form a single GDI (A+B). Typically, the subsequences have been divided where the profile transitions to another tape casting system or is over 50 layers. Further subdivision can be done if necessary to ameliorate the effect of differing layer coefficients of expansion.

For the profile shown in Figure 2, the full layup was divided into 3 subsequences. The first subsequence was layered with 22 layers of the MC44-2 tape casting formulation. The second subsequence was layered with 37 layers that spanned the range of the Mg-Cu tape formulations. The third subsequence was layered with 18 layers that spanned the range of the Cu-W tape formulations. Subsequence 1 and subsequence 2 were initially heated to 375°C in an inert environment over a period of 12 hours to remove the organic plasticizers and binders. Subsequence 3 was initially heated up to 350°C in an inert environment over a period of 45 hours to remove the organic plasticizers and binders. With all initial processing complete, subsequence 3 was vacuum hot pressed within a graphic punch and die set using the same parameters found to properly densify the Cu-W tape casting system. Processing subsequence 3 using these parameters ensures the individual layers that make up the subsequence attain the same impedance values as measured during tape characterizations. The densified subsequence 3 part along with the initially processed subsequence 2 and subsequence 1 parts were then loaded into a steel punch and die set such that the appropriate layering was maintained. This stack-up was then processed using the same parameters found to properly densify the Mg-Cu tape casting system so that subsequence 2 and subsequence 1 would properly densify and all three subsequence would be diffusion bonded together to form a single GDI. Previous experience showed that subsequence 3 would not be significantly affected by this lower temperature hot press operation.

NON-DESTRUCTIVE TEST RESULTS

The primary non-destructive test employed to evaluate a GDI is ultrasonic C-scanning. The GDI is immersed in mineral oil while a 15 MHz Panametrics transducer with a 0.75 inch focal length performs a raster scan. A data capture gate was placed on the back surface signal to measure the amplitude of the return signal. A front surface following gate was used to normalize the front surface signal timing, which can change due to out-of-flatness of the front surface. This methodology allows the data capture gate to freely move in time, maintaining a constant gate start point in relation to the front surface while the part is scanned. The amplitude raster is a measure of the amount of energy "lost" in traveling through a sample and a good indication of defects. Figure 3 shows the difference between a GDI with no defects and a GDI with a de-lamination defect. A uniform amplitude raster provides confidence the GDI is free of defects.

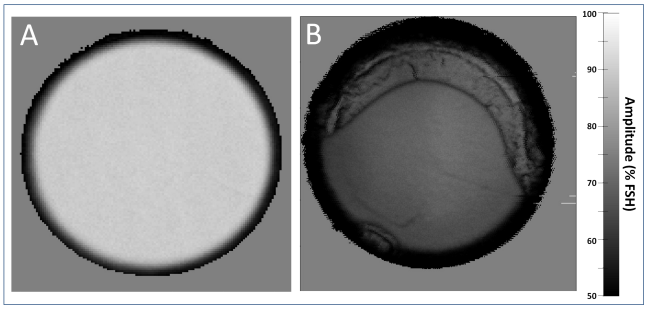

FIG. 3: C-scans of the peak amplitude of energy being reflected back from the far surfaces of 2 GDI samples: (A) a defect-free sample will create a uniform area; (B) a partially delaminated sample will create lines or areas of relatively lower peak amplitudes allowing for defects to be observed.

The front and rear surfaces of the GDI were characterized using an optical coordinate measuring machine (CMM) and an Ambios Technology XP-2 stylus profiler.

The optical CMM was used to measure flatness and parallelism. The Ambios is a calibrated instrument used to measure surface roughness, waviness, and step height with a range of 10 $\AA$ to 100 μm. Figure 4.1.2 shows typical surface profiles of a GDI with the rear and front surfaces flat to 17.8 μm and 9 μm, respectively. The optical CMM measurements were consistent with the Ambios traces.

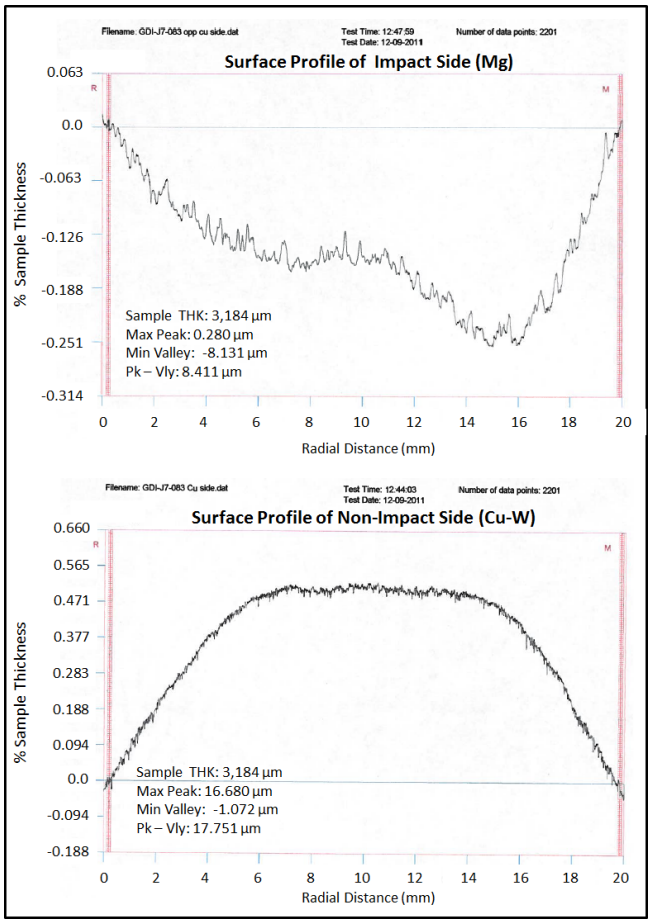

FIG. 4: Surface profilometry of GDI-J7-083 shows the impact surface is concave to less than 9 μm or 0.28% of the sample's thickness while the non-impact surface is convex to less than 18 μm or 0.57% of the sample's thickness. The sample thickness is 3.184 mm.

EXPERIMENTAL DATA

We have deployed these GDIs in gas-gun experiments to study EOS, dynamic strength and time scale at extreme conditions [6, 7]. In gas-gun experiments, an impactor is launched at a stationary target at up to 8 km/s. The target is typically made of a single or multiple step, with or without tamped LiF windows. A velocimeter (PDV [17, 18]) measures the velocity at the metal-LiF interface. These velocities are then used to extract EOSs and other rate-dependent variables. The experiments are not limited to velocity measurements, but can include optical, x-ray diffraction and other diagnostics. Here we describe a simple isentropic compression experiment for demonstration purposes.

The experimental apparatus consists of a stationary target (Figure 5) and a fast moving GDI. The target is made of a 1.75-mm flat Ta plate and a LiF crystal. Impact takes place on the Ta side of the target, and we measure particle velocity at the Ta-LiF interface. A typical velocity for GDIs is between 1 and 8 km/s. In the data presented here, the GDI was traveling at 4.86 km/s at impact, generating an initial pressure of 0.67 Mbars and a final pressure of 2.6 Mbars.

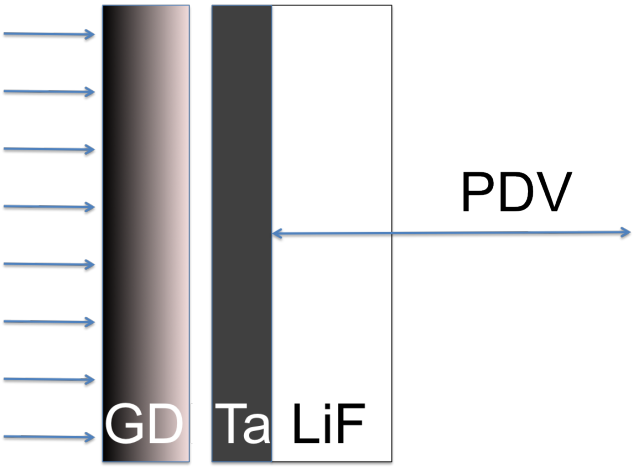

FIG. 5: Target Set-up. A graded density impactor hits the Ta-LiF target at velocity up to 8 km/s. Particle velocity at the Ta-LiF interface is recorded a velocimeter.

SIMULATION

Hydrodynamics simulation of the Ta GDI impact experiment, using the measured impedance profile of the GDI described above, have been undertaken in order to assess the performance of the GDI as well as evaluate the accuracy of the simulation approach. Simulation results for experiments of this type allow us to have confidence that the ramp compression experiment is performing as designed, and can provide for more complex analysis of experimental results which regard to the thermodynamic state of the Ta.

Each layer of the GDI has been defined in the computer simulation, with an equation of state that is formed from a linear mixing of the substituent materials (Mg, Cu, W) based upon their mole fraction. While the binary composition of each layer could be expected to have an equation of state that differs from a linear mixing rule, it has been found in past research that this simple approach captures the relevant compressive behavior.[15] The equation of

state of the Ta target and LiF window have been previously well validated in the regime accessed here, 0.5-2.5 Mbar pressure.[1, 19]

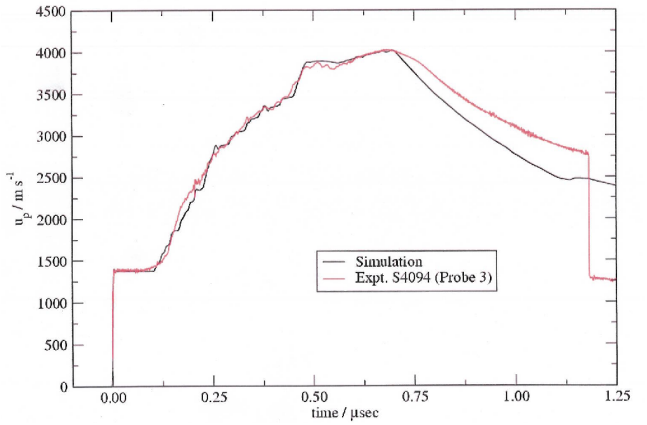

FIG. 6: Comparison of one-dimensional hydrodynamic simulation of a Ta GDI experiment and measured particle velocity. Experimental data was measured *in situ* at the Ta-LiF interface. Simulation was carried out prior to experiment.

Lagrangian hydrodynamics in 1D have been performed on a fine resolution mesh, with the initial conditions defined by the impact velocity of 4.86 km/s. The particle velocity of the Ta at the interface of the LiF window have been extracted from the simulation and compared with the experiment in Figure 6, and are found to be in excellent agreement.

CONCLUSION

Fabrication of a GDI using layers of precisely mixed Mg, Cu, and W is achievable using an A+B construction method. This raises the highest impedance of the GDI and expands the range of accessible phase space. Gas gun experiments and hydrodynamic simulations have confirmed tailoring the shock profile is possible over the entire impedance range. Future work will focus on scaling the A+B construction method to larger sized GDIs.

ACKNOWLEDGMENT

We would like to acknowledge useful discussions with N. C. Holmes, J. Haslam and the dedicated efforts of N. Hinsey, A. Ladran, C. McLean, S. Weaver, and E. White. This work was performed under the auspices of the U.S. Department of Energy by Lawrence Livermore National Laboratory under Contract DE-AC52-07NA27344

* Electronic address: yep2@llnl.gov

[1] A. C. Mitchell, W. J. Nellis, *J. Appl. Phys.* **52** (1981) 3363-3374
[2] J. H. Nguyen, N. C. Holmes *Nature* **427** (2004) 339-442
[3] V. Iota, C. S. Yoo, H. Cynn, *Science* **283** (1999) 1510-1513
[4] H. Herberhold, S. Marchal, R. Lange, C.H. Scheyhing, R.F. Vogel, R. Winter, *J. Mol. Biol..* **330** (2003) 1153-1164
[5] V. V. Struzhkin, M. I. Eremets, W. Gan, H. -K. Mao, R. J. Hemley, *Science* **298** (2002) 1213-1215
[6] J. H. Nguyen, D. A. Orlikowski, F. H. Streitz, J. A. Moriarty, N. C. Holmes, *J. Appl. Phys.* **100**, (2006) 023508
[7] J. H. Nguyen, D. A. Orlikowski, F. H. Streitz, N. C. Holmes, J. A. Moriarty, *Shock Comp. Cond. Matt.* M. D. Furnish, L. C. Chhabildas, R. S. Hixson, (eds.) (AIP Conf. Proc., Melville, New York)(2003) pp. 1225-1230.
[8] M. Eremets, *High Pressure Experimental Methods,* Oxford University Press, Oxford, (1996).
[9] Y. B. Zeldovich, Y. P. Raizer, *Physics of Shock Waves and High- Temperature Hydrodynamic Phenomena,* Academic Press, New York, (1967).
[10] C. A. Hall, *Phys. Plasma* **7** (2000) 2069-2075
[11] C. A. Hall, J. R. Assay, M. D. Knudsen, W. A. Stygar, R. B. Spielman, T. D. Pointon, D. B. Reisman, A. Toor, R. C. Cauble,, *Rev. Sci. Instrum.* **72** (2001) 3587-3595
[12] J. Edwards, K. T. Lorenz, B. A. Remington, S. Pollaine, J. Colvin, D. Braun, B. F. Lasinski, D. Reisman, J. M. McNaney, J. A. Greenough, R. Wallace, H. Louis, D. Kalantar, *Phys. Rev. Lett..* **92** (2004) 75002
[13] L. C. Chhabildas, J. R. Asay, L. M. Barker, *SAND 88-0306* Sandia National Laboratory, Albuquerque, New Mexico, (1988).
[14] L. P. Martin, D. A. Orlikowski, and J. H. Nguyen, *Mater. Sci. Eng. A* **427** (2006) 83-91
[15] L. P. Martin, J. R. Patterson, D. A. Orlikowski, and J. H. Nguyen, *J. Appl. Phys.* **102** (2007) 023507
[16] R. T. Krone, L. P. Martin, J. R. Patterson, D. Orlikowski, and J. H. Nguyen *Mater. Sci. Eng. A* **479** (2008) 300-305
[17] O. T. Strand, D. R. Goosman, C. Martinez, T. L. Whitworth, and W. W. Kuhlow *Rev. Sci. Instrum.* **77** (2006) 083108
[18] L. M. Barker, R. E. Hollenbach, *J. Appl. Phys.* **43** (1972) 4669-4675
[19] J L. Wise and L. C. Chhabildas, *Shock Waves in Condensed Matter* Plenum Press, New York, (Y. M. Gupta (ed.)) (1986) 441-454